Multi-Channel Free-Space Optics Receiver Enabled by a Programmable Photonic Processor

SeyedMohammad SeyedinNavadeh[1], Maziyar Milanizadeh[1,2], Francesco Zanetto[1], Vittorio Grimaldi[1], Christian De Vita[1], Charalambos Klitis[3], Marc Sorel[3,4], Giorgio Ferrari[1], David A.B. Miller[5], Andrea Melloni[1], Francesco Morichetti[1]

[1] Dipartimento di Elettronica, Informazione e Bioingegneria - Politecnico di Milano, Milano, 20133 Italy. (*francesco.morichetti@polimi.it*)
[2] Advanced Electronics and Photonics Research Centre, National Research Council Canada, M-50, 1200 Montreal Rd. Ottawa, ON, Canada, K1A 0R6
[3] School of Engineering University of Glasgow, Glasgow, G12 8QQ, UK [4] TeCIP Institute, Scuola Superiore Sant'Anna, 56124 Pisa, Italy
[5] Ginzton Laboratory, Stanford University, Spilker Building, Stanford, CA 94305, USA

A silicon photonic programmable processor of reconfigurable Mach-Zehnder interferometers is used to receive pairs of orthogonal spatially-overlapped beams modulated, sharing the same wavelength and polarization. The processor can automatically separate the two beams without any excess loss and no prior information on the incoming beams.

Keywords—Programmable photonic circuits, free-space optics, silicon photonics

I. INTRODUCTION

Reconfigurable and programmable photonic integrated circuits (PICs) have been recently proposed in different application fields, including manipulation of guided modes, quantum information processing and artificial neural networks [1]. Recently, we demonstrated that a silicon photonics mesh of Mach-Zehnder Interferometers (MZIs) can be effectively used to manipulate free-space optical beams and implement a number of optical functions, including beam steering, beam identification, and identification and coupling of a free space beam coming from an arbitrary direction [2].

In this work, using a "multi-row" mesh of MZIs as the photonic processor, we demonstrate loss-less separation and sorting of orthogonal mode pairs, even when these modes are indistinguishable in wavelength and polarization and are completely spatially overlapped on the mesh. We evaluate the separation quality by evaluating the penalty on two 10 Gbit/s modulated free-space channels.

II. PROGRAMMABLE PHOTONIC PROCESSOR

The programmable photonic processor employed in this work is fabricated in a silicon photonics platform (standard 220-nm-thick waveguides) and has a "diagonal" mesh architecture with MZIs as the single building block. As shown in Fig. 1(a), 8 and 7 MZIs are cascaded in the 1st and 2nd "row", respectively, to construct a 9-by-2 photonic processor. On the left side of the processor, an array of 3×3 grating couplers (placed 50 µm apart) are exploited as free-space optical receivers to couple the incoming light from free space to 9 single-mode waveguides of the processor. On the right side of the processor, the 2 top waveguides, labeled as WG_j, are connected to grating couplers for fiber optic coupling. Each single block of the processor consists of a balanced MZI (arm length of 80 µm and a width of 70 µm), with two 3-dB directional couplers (of 40 µm length and 300 nm gap). Each block can be configured by two thermo-optic actuators (heaters), made of TiN metal strips, fabricated on top of the waveguides in internal and external arms of the
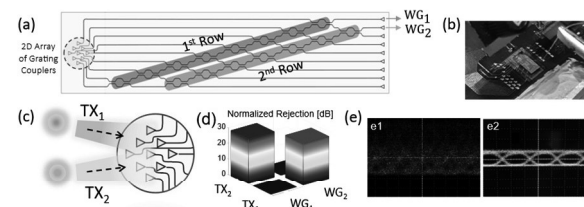
Figure 1:(a) Schematic of a 9×2 diagonal photonic processor comprising two rows of tunable MZIs and implementing a FSO mode-separator. The 2D array of grating couplers is used to couple free-space beams into the silicon waveguides. (b) Photograph of the photonic chip assembled on a PCB (c) Schematic representation of two free-space beams (TX$_1$ and TX$_2$), sharing the same wavelength and state of polarization, and arriving at the receiver from different directions. (d) Bar chart showing the normalized rejection of the beams TX$_1$ and TX$_2$ at the output waveguides WG$_1$ and WG$_2$. (e) Measured eye diagrams of two received intensity modulated 10 Gbit/s OOK signals transmitted by using the two beams TX$_1$ and TX$_2$: (e$_1$) when the photonic processor is not configured, (e$_2$) when it is reconfigured to each channel.

MZI, to give controllable phase shifts, and a transparent integrated CLIPP [3] photodetector fabricated at the lower output port of each MZI. With an appropriate electronic circuit (Fig. 1b), an automated control algorithm can be implemented for configuring each MZI block by reading out the detectors and providing proper control signals to the phase-shifters.

III. BEAMS ORTHOGONAL IN DIRECTION

Direction diversity, as a degree of freedom in the capacity of optical networks, is deployed by impinging two beams sharing the same wavelength and polarization onto the receiver from different directions. In conventional free-space systems, such an overlapping combination of the received beams would be power-split to the number of channels, with each channel reconstructed appropriately, an unavoidable splitting loss that increases with the number of channels.

In this work, by using a programmable photonic processor consisting of MZIs meshes (Fig. 1a), we can receive and split two (or more with a larger mesh) orthogonal beams impinging on the receiver. These two free-space beams (TX$_1$ and TX$_2$) share an identical Gaussian shape, wavelength (1550 nm) and polarization status (TE polarization, to match the polarization sensitivity of the grating couplers) and are shone from two different directions onto the 2D array of grating couplers of the processor (Fig. 1c) with a relative angle of 1.25°. The mesh is self-configured by exploiting a local feedback control of each MZI block, which minimizes power of the beam at the monitor detectors in each row using the two thermo-optic phase shifters. Although both incoming beams co-propagate inside the waveguides of the processor,

they can be identified by the detectors provided that they are marked with suitable labels (pilot tones) superimposed as a shallow amplitude modulation at two different frequencies. Upon self-configuration of the rows of the photonic processor to extract each transmitted beam, identical optical powers from two transmitters are measured at ports WG_1 (from TX_1) and WG_2 (TX_2), which is reported as 0 dB normalized rejection in the bar chart of Fig. 1(d). More than 25 dB optical crosstalk suppression, i.e., power of TX_1 in WG_2 and TX_2 in WG_1, is recorded and reported in the same bar chart. If we swap the mode sorting status, meaning coupling TX_2 to WG_1 and TX_1 to WG_2, the same level of optical isolation is observed. Such a low crosstalk level allows two free-space optical modulated channels to be received and sorted at the output waveguides. As an exercise, two 10 Gbit/s on-off keying (OOK) signals are shone onto the chip and eye diagrams of the recovered channels are recorded for each WG port; these are shown in Fig. 1(e_1) for an arbitrary status of the receiver (before self-configuration) and the eye diagrams of TX_1 and TX_2 at port WG_1 are severely overlapped. Upon configuration of the mesh rows for both channels the same eye diagrams are recorded at output WG ports (Fig. 1e_2), showing now an "open" eye.

IV. MODE DIVERSITY IN PERTURBING CHANNEL

In principle, any set of orthogonal modes can be sorted and split using the photonic mesh processor [4]. In [5], we demonstrated that two spatially overlapping modes (coming from the same angle) with same wavelength and state of polarization can be split and sorted based on this concept. There, we adopted fundamental and first higher order Hermite-Gaussian-like modes and we demonstrated that two modulated channels can be sorted out without any penalty by evaluating the recorded eye diagrams at output WG ports.
In this work, we extend this concept to a particular case of two spatially overlapping modes propagating through a mode mixing obstacle or a free-space path perturbation. Mathematically, the linear transformation performed by the mode mixer, which maps the original orthogonal modes to another pair of orthogonal modes, can be inverted by the

processor. $Mask_1$ in Fig. 2(a), which is a -45°-rotated 0-π phase mask, is used to transform a fundamental Hermite-Gaussian mode ($Mode_1$) to the first higher order HG_{10}-like mode ($Mode_2$) that is rotated -45°. This mode overlaps spatially with the fundamental mode after passing through the beam splitter and propagates towards the chip. An additional 0-π phase mask ($Mask_2$ in Fig. 2a) performs a linear transformation between pairs of orthogonal modes impinging on the mesh. In this scenario, the mask converts the fundamental mode HG_{00} into a +45°-rotated HG_{10}-like mode ($Mode_3$), while the higher-order mode HG_{10}-like mode (-45°-rotated) is transformed to a 45°-rotated HG_{11}-like ($Mode_4$).
Nothing changes in the operation required to separate these new modes. The automatic reconfiguration needs no a-priori information on the shape of the incoming beams. The processor is reconfigured to extract $Mode_3$ at output port WG_1 and $Mode_4$ at output port WG_2. Measuring powers of the extracted modes at each output port (Fig. 2b), we see > 30 dB mutual isolation. High-quality mode separation is seen when the processor is used as a two-mode-separator receiver in a data transmission link, where each mode carries a 10 Gbit/s intensity-modulated OOK signal. Neither distortion nor inter-symbol interference effects are visible in the received eye diagrams of Fig. 2(c) for the extracted channels at the output WG ports. Fig. 2(d) shows the bit error rate (BER) vs. optical signal to noise ratio (OSNR) measured on the data channels separated by the receiver. With respect to the reference blue curve (i.e., when shining only $Mode_3$ (and extracting at WG_1) in absence of $Mode_4$, given by the BER curves of $Mode_3$ extracted at WG_1 (yellow curve) and $Mode_4$ at WG_2 (purple curve)) no OSNR penalty is observed once both data channels are transmitted and are sorted out by the processor. These results validate the effectiveness of the processor for separating generic pairs of orthogonal modes emerging from a free-space mode converter.

V. CONCLUSIONS

We demonstrated that using a programmable photonic processor based on meshes of MZIs, we can separate and sort out generic pairs of orthogonal modes spatially overlapped in the free space. No prior information is needed for the processor the be reconfigured and we examine this concept by evaluating quality of the received modulated free-space channels sharing the same wavelength and polarization.

Figure 2: (a) Schematic representation of two free-space modes ($Mode_3$ and $Mode_4$) that arrive on the receiver after a mode conversion performed by a 45°-rotated phase $Mask_2$. In the reported experiment, $Mode_3$ and $Mode_4$ correspond to 45°-rotated HG_{10}-like and HG_{11}-like modes, respectively, resulting from mode conversion of $Mode_1$ and $Mode_2$. $Mode_2$ is a HG_{10}-like mode -45°-rotated and generated by passing the fundamental mode through the phase $Mask_1$. (b) Bar chart showing the normalized insertion loss of the $Mode_3$ and $Mode_4$ at the output waveguides WG_1 and WG_2. (c) Measured eye diagrams of two intensity modulated 10 Gbit/s OOK signals transmitted by using $Mode_3$ and $Mode_4$ for the configurations considered in (b). (d) BER measurements of 10 Gbit/s OOK channels simultaneously transmitted in the free space on spatially overlapped modes ($Mode_3$ and $Mode_4$) and separated by the photonic processor. Yellow and purple curves indicate the BER measured for each of extracted $Mode_3$ and $Mode_4$, respectively, while blue curve is the reference curve for only $Mode_3$ extracted.

REFERENCES

[1] W. Bogaerts, D. Pérez, J. Capmany, et al. "Programmable photonic circuits," Nature 586, 207–216, 2020.

[2] M. Milanizadeh, F. Toso, G. Ferrari, et al. "Coherent self-control of free-space optical beams with integrated silicon photonic meshes," Photon. Res. 9, 2196-2204, 2021.

[3] F. Morichetti, et al, "Non-invasive on-chip light observation by contactless waveguide conductivity monitoring," J. Selected Topics in Quantum Electronics, vol. 20, no. 4, Jul./Aug. 2014.

[4] David A. B. Miller, "Self-aligning universal beam coupler," Opt. Express 21, 6360-6370 (2013).

[5] S. SeyedinNavadeh et al., "Self-Configuring Silicon-Photonic Receiver for Multimode Free Space Channels," 2021 IEEE 17th International Conference on Group IV Photonics (GFP), 2021.